

# Time-Resolved EPR and Optical Studies of Intermoiety Interactions in the Lowest Triplet State of L-Shaped Dimers of Naphthalene: Conformation Dependence of Excitation Exchange Interaction

Masahide Terazima,<sup>†</sup> Jianjian Cai,<sup>‡</sup> and Edward C. Lim<sup>\*,‡,§</sup>

Department of Chemistry, Kyoto University, Kyoto 606, Japan, and Department of Chemistry, The University of Akron, Akron, Ohio 44325-3601

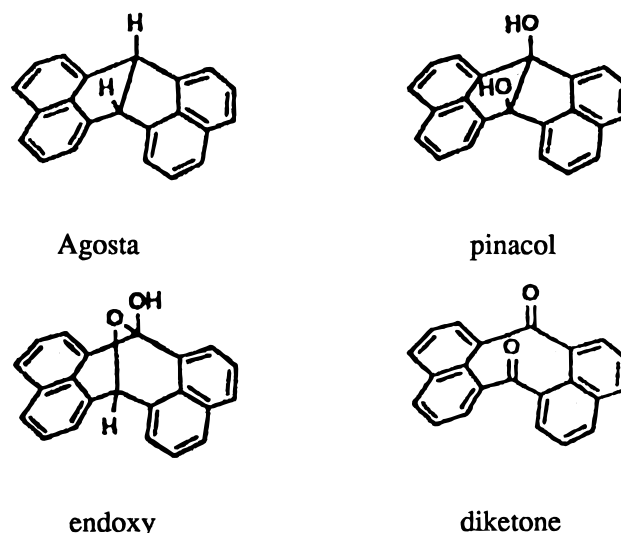
Received: October 12, 1999; In Final Form: January 4, 2000

Time-resolved EPR (TREPR), transient absorption, and phosphorescence spectra have been measured in solid matrixes at 77 K for the covalently linked L-shaped dimers of naphthalene, in which the in-plane long axes of the two naphthalene moieties are parallel and the in-plane short axes make an angle. The zero-field splitting (ZFS) parameters obtained by simulation of the TREPR spectra are consistent with the dimer geometries, if it is assumed that excitation exchange interaction is responsible for the small  $D$  values of the dimers relative to the monomer. The tilt angle in the triplet state is significantly smaller for the dimers exhibiting excimeric phosphorescence than those exhibiting monomeric emission. Comparison of the spectral position and lifetime of phosphorescence from the L-shaped dimers with those from the sandwich dimers indicates that the excitation exchange interaction is substantially greater for the L-shaped dimers as compared to the sandwich dimers. The proposal that the preferred conformation of the triplet excimer of naphthalene is L-shaped, rather than sandwich, is supported by the measurements.

## I. Introduction

Transannular interactions in the covalently linked aromatic dimers are important for the understanding of the conformation of aromatic excimers and the nature of the intermolecular forces responsible for excimer formation. Of particular importance has been the discovery that, of  $\alpha,\omega$ -diphenylalkanes<sup>1</sup> and  $\alpha,\omega$ -dinaphthylalkanes,<sup>2</sup> only the species with trimethylene link exhibits broad, red-shifted, fluorescence that can be attributed to an intramolecular singlet excimer (Hirayama's  $n = 3$  rule). Since only the species linked by a three-atom bridge can adopt a face-to-face arrangement of the two aromatic moieties, the observation led to a conclusion that the preferred conformation of the singlet excimer is a sandwich-pair geometry. The face-to-face sandwich structure of the singlet excimer supports the theoretical conclusions<sup>3–7</sup> that the species derive their stability from charge resonance and exciton resonance. For the triplet excimers of aromatic hydrocarbons, both the exciton and charge resonance mechanisms are expected to be less important for two reasons. First, since the electronic transition from the ground state to the triplet state is only weakly allowed, the exciton resonance (which scales with the square of the transition moment) would be substantially smaller for the triplet excimer as compared to the singlet excimer. Moreover, the charge resonance is also expected to be smaller relative to the corresponding singlet excimer, as the lowest triplet state is energetically farther removed from the intermoleity charge-transfer (CT) excited state. These considerations led to a proposal<sup>8,9</sup> that van der Waals forces contribute significantly to the stability of the triplet excimer. Thus, the conformational structure of the triplet excimer may resemble the geometry of the ground-state dimer, rather than that of the singlet excimer.<sup>9</sup>

SCHEME 1: Molecular Structures and Designations of the L-Shaped Dimers Used in the Time-Resolved EPR and Optical Studies



A striking confirmation of the structural difference between the singlet and triplet excimers comes from the observation of excimer phosphorescence from dinaphthylmethanes<sup>10</sup> and dinaphthyl ethers<sup>10</sup> that cannot adopt a face-to-face sandwich arrangement of the two naphthalene rings. Moreover, the sandwich dimer of naphthalene (produced by photolytic dissociation of the photodimer in rigid glass at 77 K) exhibits monomeric phosphorescence despite the fact that its fluorescence is distinctly excimer-like.<sup>2</sup> Because the room-temperature phosphorescence<sup>8,11</sup> and the triplet–triplet absorption<sup>12,13</sup> spectra of naphthalene and dinaphthylalkanes are similar to those of the Agosta dimers<sup>14</sup> of  $C_{2v}$  symmetry (see Scheme 1 for the

<sup>†</sup> Kyoto University.

<sup>‡</sup> The University of Akron.

<sup>§</sup> Holder of the Goodyear Chair in Chemistry at The University of Akron.

structures), it was proposed<sup>8,9,11</sup> that the likely geometry of the triplet excimer is an L-shaped (or a butterfly) structure, in which the long in-plane axes of the two naphthalene moieties are nearly parallel and the short in-plane axes make an angle. The preference for the L-shaped structure of the naphthalene triplet excimer has been interpreted<sup>8,9</sup> as a compromise between the dispersion force, which favors a cofacial structure, and the electrostatic force (quadratic–quadratic interaction) which favors a T-shaped structure.

A strong conformational dependence of intermolecular interactions in the L-shaped dimers of naphthalene is suggested by the fact that the ability for the dimers to exhibit excimer phosphorescence appears to be sensitively dependent on the flexibility of the molecule. Thus, while the diketone and endoxy dimers exhibit excimeric phosphorescence, the more rigid Agosta and pinacol dimers display monomeric phosphorescence, in rigid glass at 77 K.<sup>11,15</sup>

To explore the structure of the T<sub>1</sub> dimer and the conformational dependence of the intermolecular interactions, we have carried out time-resolved EPR (TREPR) and optical measurements on various L-shaped dimers of naphthalene with differing conformational flexibility, for comparison with each other as well as with the sandwich dimers of naphthalene. The results indicate that the excitation exchange interaction is substantially greater for the L-shaped dimers than for the sandwich dimers. The conclusion<sup>8,9,11</sup> that the preferred geometry of the triplet excimer of naphthalene is L-shaped, and not a sandwich, is therefore supported by the measurements.

## II. Experimental Section

The phosphorescence and polarized emission spectra were measured in rigid glass at 77 K with an Aminco SPF-500 spectrofluorometer. The laser-induced transient absorption spectra were recorded using the diode-array spectrometer described in detail elsewhere.<sup>10a</sup> The sample concentration of 10<sup>-4</sup> mole dm<sup>-3</sup> was typically used in the experiment.

The TREPR measurements at 77 K were made using the apparatus previously described.<sup>16</sup> Briefly, a sample in a cylindrical cavity, of concentrations of 10<sup>-2</sup>–10<sup>-3</sup> mol dm<sup>-3</sup>, was irradiated by an excimer laser (Lumonics EX-400) with a XeCl fill ( $\lambda = 308$  nm,  $\sim 100$  mJ/pulse) at a repetition rate of 12 Hz. Transient EPR signal was detected with a conventional EPR spectrometer (JEOL FE3X) with a fast response preamplifier. The signal was amplified and integrated by a boxcar integrator (PAR model 160). The TREPR spectra were interpreted by the spin Hamiltonian

$$\begin{aligned} H &= g\beta\mathbf{B}\cdot\mathbf{S} + \mathbf{S}\cdot\mathbf{D}\cdot\mathbf{S} \\ &= g\beta\mathbf{B}\cdot\mathbf{S} - XS_x^2 - YS_y^2 - ZS_z^2 \\ &= g\beta\mathbf{B}\cdot\mathbf{S} + D[S_z^2 - (1/3)S^2] + E(S_x^2 - S_y^2) \end{aligned} \quad (1)$$

where  $\mathbf{D}$  is the ZFS tensor with principal values,  $X$ ,  $Y$ , and  $Z$ , and  $D$  and  $E$  describe the ZFS parameters that are related to the principle values by

$$\begin{aligned} D &= -X + (Y + Z)/2 = -3/2X \\ E &= (Y - Z)/2 \end{aligned} \quad (2)$$

A computer program simulated the observed TREPR spectra, by assuming the line shape to be Gaussian type of width 8 mT.

The samples of the L-shaped dimers of naphthalene were synthesized and purified following the procedures of Agosta.<sup>14</sup> The molecular structures of the various L-shaped dimers and

our designation of them are given in Scheme 1. To prevent photochemical dehydrogenation of the pinacol dimer to the diketone dimer,<sup>15</sup> both the TREPR and optical measurements of the pinacol dimer were carried out in ethanol glass at 77 K.

## III. Results

**a. Phosphorescence Spectra.** Figure 1 displays the phosphorescence spectra of the various L-shaped dimers of naphthalene in rigid glass at 77 K. It should be noted that while the Agosta and the pinacol dimers exhibit the structured emission resembling the naphthalene monomer phosphorescence, the endoxy and the diketone dimers display the less structured, and red shifted, emission that has been assigned to the excimer phosphorescence. The spectral broadening and red shift of the dimer phosphorescence, relative to the monomer phosphorescence of naphthalene, is the largest for the diketone dimer and the smallest for the Agosta dimer. Thus, the emission frequency decreases in the order Agosta dimer > pinacol dimer > endoxy dimer  $\geq$  diketone dimer, paralleling the order in molecular flexibility. As previously reported,<sup>11</sup> the phosphorescence lifetimes of the endoxy and diketone dimers are very short (milliseconds) relative to naphthalene ( $\sim 2.6$  s) and acenaphthene ( $\sim 2.6$  s). Since the quantum yield of phosphorescence is not significantly different for the L-shaped dimers as compared to that of monomer (naphthalene or acenaphthene),<sup>17</sup> we may conclude that T<sub>1</sub>  $\rightarrow$  S<sub>0</sub> radiative and nonradiative decay rates are much greater for the L-shaped dimers than for the corresponding monomer.

Interestingly, the spectral position of the excimeric phosphorescence from the diketone and endoxy dimers shifts to longer wavelengths when the viscosity of the glassy solvent is decreased. Thus, in a series of mixed solvents containing different volume percent of isopentane and methylcyclohexane, the peak wavelength of the endoxy dimer phosphorescence changes continuously from 503 nm in pure methylcyclohexane (hardest glass) to 520 nm in pure isopentane (softest glass). The 520 nm corresponds to the peak wavelength of the excimer phosphorescence of the dimer in fluid hydrocarbon solvents at room temperature. These results strongly suggest that the L-shaped dimers undergo significant light-induced conformational change in glassy matrixes at 77 K. As reported previously,<sup>11</sup> the room-temperature phosphorescence of the L-shaped dimers are all excimer-like, and they closely resemble the phosphorescence of the diketone dimer at 77 K.

In contrast to the endoxy and diketone dimers, the dimers with face-to-face arrangement of the naphthalene moieties exhibit monomer-like phosphorescence with relatively long lifetimes. Thus, the sandwich dimer of naphthalene,<sup>2</sup> naphthalene-annelated dimer,<sup>18</sup> and naphthalenophanes<sup>19,20</sup> all exhibit phosphorescence that closely resembles the phosphorescence of naphthalene, both with respect to the spectral position and lifetime ( $\sim 2$  s).

**b. Transient Absorption Spectra.** Figure 2 presents the laser-induced triplet–triplet absorption spectra of the pinacol and endoxy dimer in ethanol glass at 77 K. Unlike acenaphthene or naphthalene, which exhibit only the characteristic triplet–triplet absorption of the monomer at about 425 nm,<sup>21</sup> the pinacol dimer, the endoxy dimer, and the diketone dimer exhibit, in addition, an intense absorption at about 600 nm (the Agosta dimer was unfortunately not available for the time-resolved absorption or the TREPR study). The shorter wavelength feature of the dimers at about 430 nm is due to the triplet–triplet absorption of the locally excited (LE) state, whereas the longer wavelength feature at about 600 nm is the intermolecular <sup>3</sup>A<sub>1</sub> ←

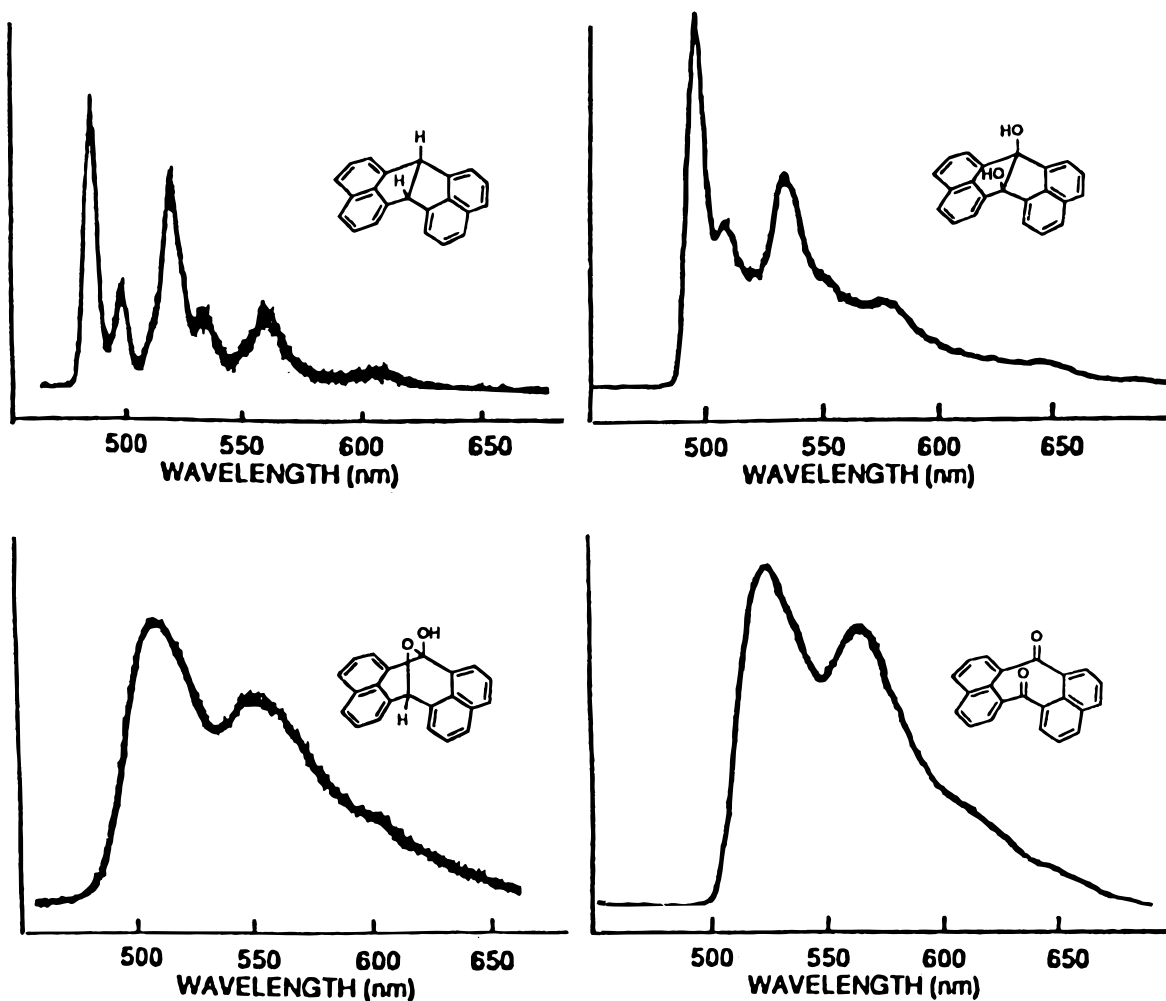


**Figure 1.** Phosphorescence spectra of the L-shaped dimers in rigid glass at 77 K. The solvent was ethanol for the pinacol dimer and methylcyclohexane for the rest.

$^3B_2$  (or  $^3\delta \leftarrow ^3\sigma$  in the notation of Chandra and Lim<sup>7</sup>) CT transition<sup>7,20,22</sup> from the lowest energy exciton resonance state to the lowest energy charge resonance state. For each dimer, the LE and CT absorption systems decay with rates which are identical to each other, and to the decay rate of the respective phosphorescence.<sup>23</sup> The intermoiety CT absorption has also been observed for dinaphthylmethanes,<sup>10</sup> dinaphthyl ethers,<sup>10</sup> naphthalene-annelated dimers,<sup>13</sup> quinoxaline-annelated dimer,<sup>13</sup> naphthalenophans,<sup>24</sup> and the sandwich dimer of naphthalene.<sup>23</sup> We may therefore conclude that, the transient absorption spectra reveal the intermoiety interaction leading to the stabilization of triplet excimer, even for systems that exhibit monomeric phosphorescence.

**c. TREPR Spectra.** To clarify the triplet character of the monomer, the TREPR spectrum of acenaphthene was analyzed under conditions identical to those for the L-shaped dimers. Figure 3a shows the TREPR spectrum of randomly oriented acenaphthene in toluene at 0.5  $\mu$ s after the laser irradiation at 77 K. The  $\Delta m = \pm 1$  transitions display the spin polarization pattern of EEA/EAA, where E and A represent emission and absorption of microwave, respectively. The observed spectrum can be reproduced with ZFS parameters of  $X = -0.0648$   $\text{cm}^{-1}$ ,  $Y = 0.0472$   $\text{cm}^{-1}$ ,  $Z = 0.0176$   $\text{cm}^{-1}$ , and the ratio of the relative population difference of  $(P_Y - P_X)/(P_Z - P_X) = 1.0:0.4$ . The zero-field sublevels and principal axes for acenaphthene and the L-shaped dimers of naphthalene are given in Figure 4. Alternative parameters  $X = 0.0648$   $\text{cm}^{-1}$ ,  $Y = -0.0472$   $\text{cm}^{-1}$ ,

$Z = -0.0176$   $\text{cm}^{-1}$ ,  $(P_X - P_Y)/(P_Z - P_Y) = 1.0:0.6$ , which also reproduce the observed spectrum, can be excluded by considering the expected similarity of the triplet character of acenaphthene to that of naphthalene. The observed TREPR spectrum of acenaphthene in ethanol is very similar to that in toluene, indicating the absence of significant solvent effect.

Figure 3b shows the TREPR spectrum of the pinacol dimer in ethanol. The spectrum exhibits a AEA/EAE polarization pattern, and it can be simulated with the parameters  $X = -0.0491$   $\text{cm}^{-1}$ ,  $Y = 0.0417$   $\text{cm}^{-1}$ ,  $Z = 0.0074$   $\text{cm}^{-1}$ ,  $(P_Y - P_Z)/(P_X - P_Z) = 1.0:1.0$ , or  $X = -0.0417$   $\text{cm}^{-1}$ ,  $Y = 0.0491$   $\text{cm}^{-1}$ ,  $Z = -0.0074$   $\text{cm}^{-1}$ ,  $(P_Y - P_Z)/(P_Z - P_X) = 1.0:1.0$ , Figure 3b. Since the simulated spectra using these two sets of parameters are equivalent, the question of which set is the correct cannot be answered from the observed spectrum alone (vide infra). As expected from the photochemical conversion of the pinacol dimer to the diketone dimer in aprotic solvents,<sup>15</sup> the TREPR spectrum of the pinacol dimer in toluene is identical to that of the diketone dimer (vide infra) in the same solvent.

The TREPR spectrum of the endoxy dimer in toluene, Figure 3c, can be analyzed by assuming two overlapping spectra (broad and sharp). The ZFS and population ratio of the endoxy dimer are  $X = -0.049$   $\text{cm}^{-1}$ ,  $Y = 0.030$   $\text{cm}^{-1}$ ,  $Z = 0.059$   $\text{cm}^{-1}$ ,  $(P_Y - P_X)/(P_Z - P_X) = 0.8:1.0$ , or  $X = -0.030$   $\text{cm}^{-1}$ ,  $Y = 0.049$   $\text{cm}^{-1}$ ,  $Z = -0.019$   $\text{cm}^{-1}$ ,  $(P_Y - P_X)/(P_Z - P_X) = 1.0:0.7$  for species 1 (with sharp spectrum), and  $X = -0.055$   $\text{cm}^{-1}$ ,  $Y = 0.039$   $\text{cm}^{-1}$ ,  $Z = 0.016$   $\text{cm}^{-1}$ ,  $(P_Y - P_X)/(P_Z - P_X) = 1.0:0.2$

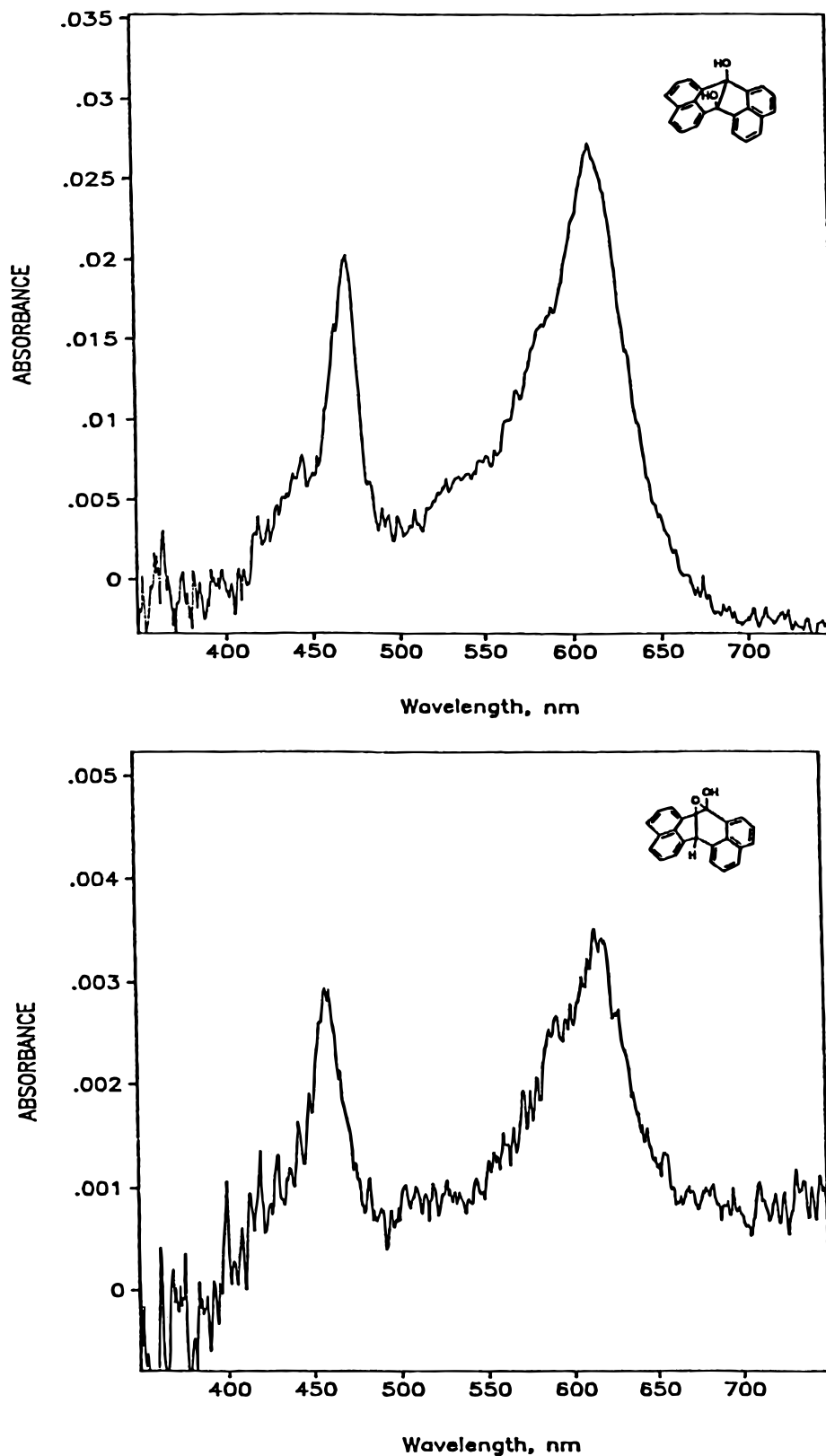
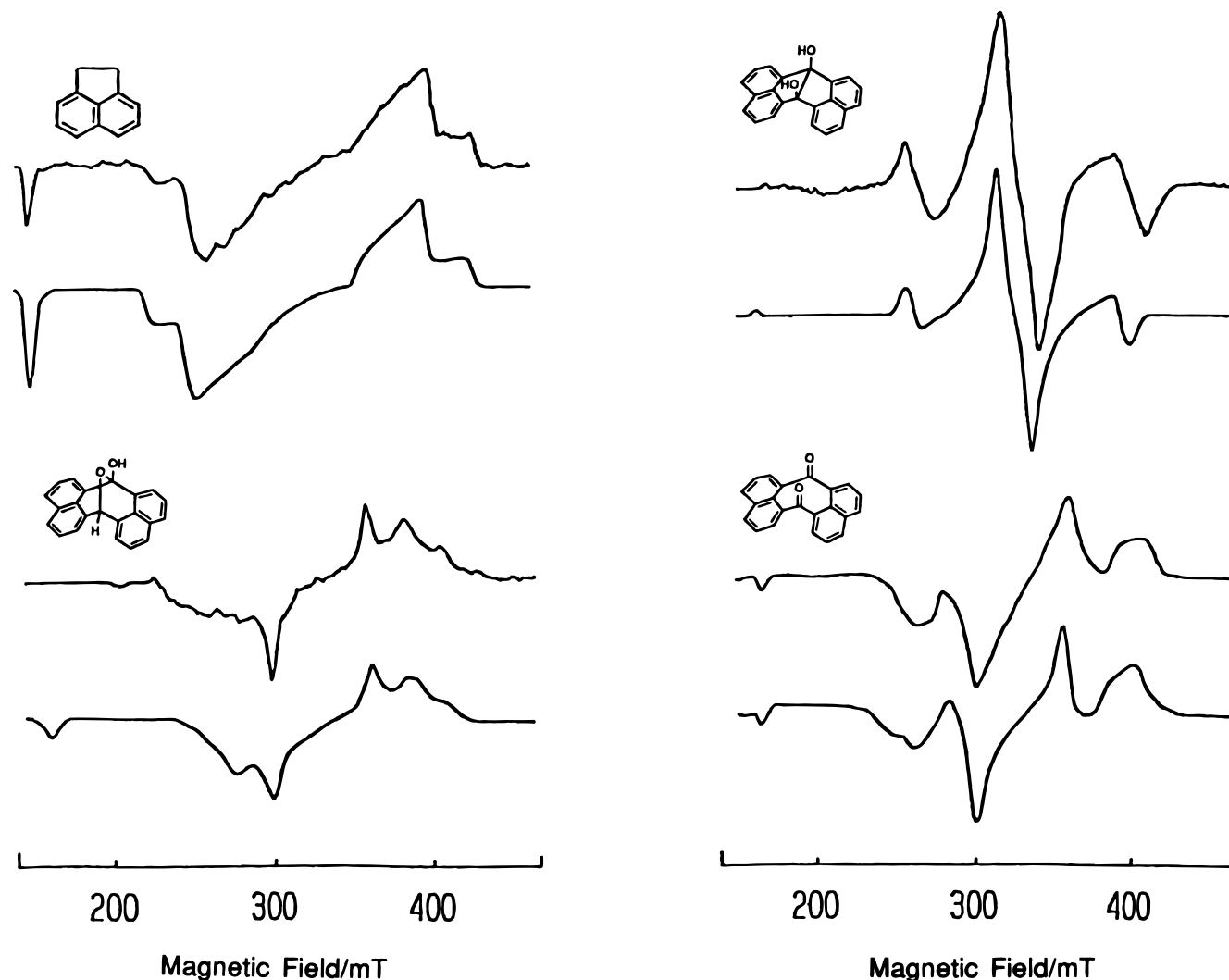


Figure 2. Transient absorption spectra of the pinacol dimer and the endoxy dimer in ethanol glass at 77 K.

or  $X = -0.039 \text{ cm}^{-1}$ ,  $Y = 0.055 \text{ cm}^{-1}$ ,  $Z = -0.016 \text{ cm}^{-1}$ ,  $(P_Y - P_X)/(P_Z - P_X) = 1.0:0.8$  for species 2 (with broad spectrum) with intensity ratio 1.5:1.0. Species 2 in the endoxy dimer is likely a product of photodecomposition, which is formed upon prolonged irradiation.

Figure 3d presents the TREPR spectrum of the diketone dimer in toluene. The  $\Delta m = \pm 1$  transition shows a complicated polarization pattern (EAE(A)/(E)AEA), and there are two  $\Delta m = \pm 2$  transitions in the lower magnetic field. These features again indicate that there are two species giving rise to the



**Figure 3.** Measured (top) and simulated (bottom) time-resolved EPR spectra of acenaphthene in ethanol, pinacol dimer in ethanol, endoxy dimer in toluene, and diketone dimer in toluene.

TREPR signal. The ZFS parameters and the ratio of the relative population differences are  $X = -0.048 \text{ cm}^{-1}$ ,  $Y = 0.031 \text{ cm}^{-1}$ ,  $Z = 0.017 \text{ cm}^{-1}$ ,  $(P_Y - P_Z)/(P_Z - P_X) = 0.3:1.0$  or  $X = -0.031 \text{ cm}^{-1}$ ,  $Y = 0.048 \text{ cm}^{-1}$ ,  $Z = -0.017 \text{ cm}^{-1}$ ,  $(P_Y - P_Z)/(P_X - P_Z) = 1.0:0.7$  for species 1, and  $X = -0.084 \text{ cm}^{-1}$ ,  $Y = 0.054 \text{ cm}^{-1}$ ,  $Z = 0.030 \text{ cm}^{-1}$ ,  $(P_Y - P_Z)/(P_X - P_Z) = 1.0:0.6$  or  $X = -0.054 \text{ cm}^{-1}$ ,  $Y = 0.084 \text{ cm}^{-1}$ ,  $Z = -0.030 \text{ cm}^{-1}$ ,  $(P_Y - P_X)/(P_Z - P_X) = 0.4:1.0$  for species 2.

Although there is more than one species, and more than one set of the ZFS parameters, that reproduces the observed TREPR spectrum, the ZFS of the L-shaped dimers can be determined by elimination. First, only the set of ZFS parameters that yield  $D$  (or  $X$ ) values smaller than that of the monomer need to be considered since the exciton hopping and charge transfer in the dimer is expected to lead to a reduction in the  $D$  value. Second, of the two sets of the ZFS parameters that reproduce the observed EPR spectrum, Figure 4, the set with two positive ZFS (scheme A) can be eliminated based on the dimer geometry (vide infra). Third, for the endoxy and diketone dimers which display both the sharp (species 1) and broad (species 2) TREPR spectra, only the species 1, with  $Y$  value very similar to that of the monomer (acenaphthene), is consistent with the dimer geometry. The  $D$  and the principal values ( $X$ ,  $Y$ , and  $Z$ ) of the ZFS parameters, based on these criteria, are listed in Table 1, together with those for acenaphthene.

When the intermolecular excitation exchange is rapid on the time scale of the TREPR experiment, the principal values of the ZFS of the L-shaped dimers are given by

$$\begin{aligned} X &= X' \cos^2(\theta/2) + Z' \sin^2(\theta/2) \\ Y &= Y' \\ Z &= Z' \sin^2(\theta/2) + X' \cos^2(\theta/2) \end{aligned} \quad (3)$$

where  $X'$ ,  $Y'$ , and  $Z'$  represent ZFS parameters of the monomer. If the ZFS of scheme A in Figure 4 represented those of the dimers correctly, the  $Z$  axes of the two monomers would have to be nearly parallel to each other, whereas  $X$  and  $Y$  tilt slightly. Since such conformation is impossible for the L-shaped dimers, scheme A can be eliminated from consideration. Conformations consistent with the dimer  $S_0$  geometries are indicated by the ZFS of scheme B. According to this scheme, each dimer has the  $Y$  axis (i.e., the in-plane long axis) of the monomer parallel and the two naphthalene moieties are rotated in the  $XZ$  plane. The tilt angle  $\theta$  (i.e., the angle between the two in-plane short axes of the monomers) for the triplet state can be calculated by using the observed ZFS and eq 3. The  $\theta$  values so obtained are close to the tilt angles expected based on the ground-state dimer geometry. The results, summarized in Table 2, demonstrate that the ZFS of scheme B correctly represent the triplet spin sublevels

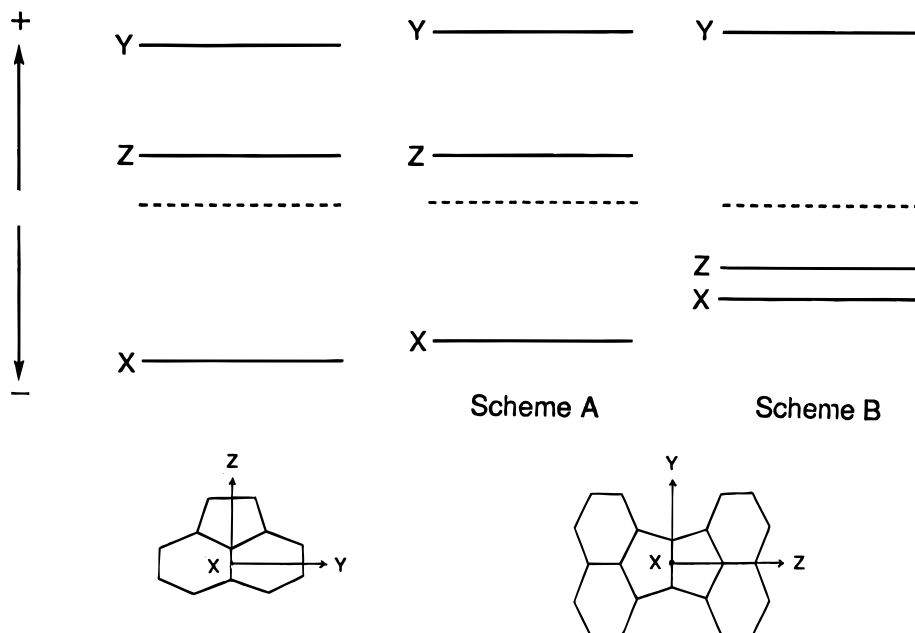


**Figure 4.** Zero-field sublevels and principal axes for acenaphthene and the L-shaped dimer. Schemes A and B for the dimer represent the two sets of ZFS parameters that reproduce the observed TREPR spectra. Only scheme B is compatible with the dimer geometry (see text).

**TABLE 1: Tilt Angles for the Lowest Triplet State of the L-Shaped Dimers of Naphthalene, Obtained from the TREPR Measurements at 77 K**

dimer/solvent <sup>a</sup>	$\theta$ (degree)
pinacol/ethanol	112
endoxy/toluene (species 1)	98
diketone/toluene (species 1)	100

<sup>a</sup> See Scheme 1 for dimer structures.

**TABLE 2: The ZFS Tensor ( $D$ ) and Its Principal Values ( $X$ ,  $Y$ , and  $Z$ ), in  $\text{cm}^{-1}$ , for the Monomers and L-Shaped Dimers of Naphthalene**

compound/solvent	$X$	$Y$	$Z$	$D^a$
acenaphthene/toluene	-0.065	0.047	0.018	0.098
pinacol dimer <sup>b</sup> /ethanol	-0.042	0.049	-0.007	0.074
endoxy dimer <sup>b</sup> /toluene (species 1)	-0.030	0.049	-0.019	0.045
diketone dimer <sup>b</sup> /toluene (species 1)	-0.031	0.048	-0.017	0.047

<sup>a</sup>  $D = -(\frac{3}{2})X$ . <sup>b</sup> See Scheme 1 for dimer structures.

of the dimers and that the excitation exchange occurs rapidly on the time scale of the EPR experiment ( $\sim 9$  GHz). Table 2 also reveals that the tilt angle is smaller for dimers exhibiting excimeric phosphorescence than the dimer displaying monomeric emission (i.e., pinacol dimer).

#### IV. Discussion

The binding in triplet excimers results from the combination of van der Waals (vdW) energy, exciton resonance (excitation exchange), and charge resonance

$$E = E_m + E_{\text{vdW}} + E_{\text{er}} + E_{\text{cr}} \quad (4)$$

where  $E_m$  represents the energy of the triplet monomer. The locally excited (LE) and charge-transfer (CT) states of the dimer are lowered by attractive vdW forces, split respectively by excitation resonance and charge resonance, and interact with each other via configuration interaction to yield the final dimer triplet states,<sup>25</sup> Figure 5. Because of the large electronic energy gap between the CT and the LE triplet states<sup>26</sup> (The Franck-Condon intensity maximum of the  ${}^3\delta \leftarrow {}^3\sigma$  CT transition is at

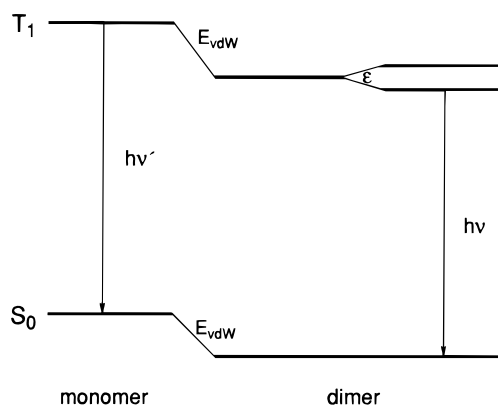


**Figure 5.** Schematic energy level diagram illustrating a dissection of the interactions in the naphthalene dimer. The triplet state of the dimer is stabilized by attractive van der Waals forces and split by exciton resonance ( $2\epsilon$ ). Configuration interaction between the locally excited triplet state and charge resonance state is not included for energetic reason (see text and note 26). The vertical arrows represent the radiative transitions (phosphorescence) from the lowest triplet state of the monomer and dimer.

about 600 nm, or  $\sim 17\,000\text{ cm}^{-1}$ , Figure 2), the configuration interaction between the two states is expected to be quite small. Consequently, the CT stabilization of the lowest triplet ( $T_1$ ) state of the dimer can be assumed to be small as compared to the stabilization by excitation exchange interaction. The small CT character of the  $T_1$  state of the L-shaped naphthalene dimer is indicated by TREPR, since the geometries of the dimers can be reproduced from the ZFS parameters by considering only the exciton resonance (section IIIc). Moreover, the intensity ratio of the LE to the intermoeity CT bands in the transient absorption spectra is essentially identical for the pinacol dimer exhibiting the monomeric phosphorescence and the endoxy (and diketone) dimer exhibiting excimeric phosphorescence (section IIIc). Since the intensity ratio is predicted to be strongly dependent on the CT character of  $T_1$  on theoretical grounds,<sup>22</sup> the result implies that there is either very little CT character in  $T_1$  or the CT character of  $T_1$  is essentially identical for the two classes of the L-shaped dimers. In either case, the CT cannot be the source

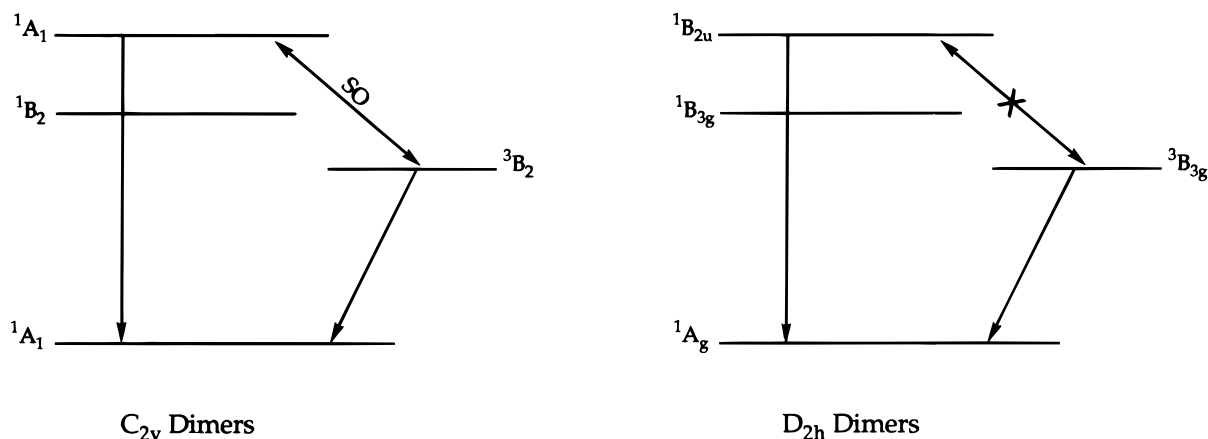


**Figure 6.** Spin-orbit coupling of the lowest  $\pi\pi^*$  triplet state with the low-lying  $\pi\pi^*$  singlet states for the L-shaped dimers of  $C_{2v}$  symmetry (left) and the sandwich dimers of  $D_{2h}$  symmetry (right). Note that, whereas the  $T_1(^3B_2)$  state of the  $C_{2v}$  dimer can effectively couple with the  $^1A_1$  state, the  $T_1(^3B_{3g})$  state of the  $D_{2h}$  dimers cannot couple with the corresponding singlet state. Only the excited singlet state of the dimers corresponding to the HOMO $\rightarrow$ LUMO transition of the monomer are indicated.

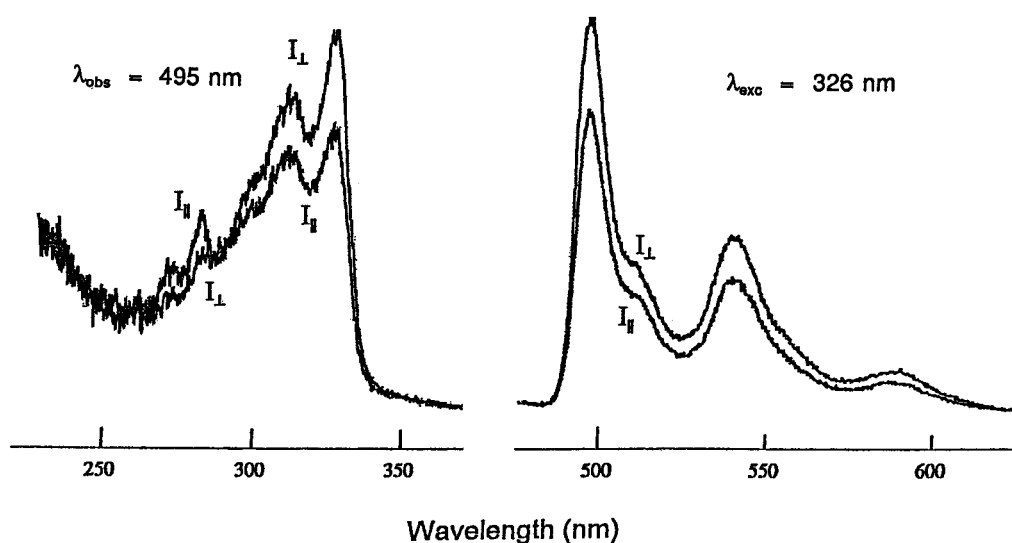


**Figure 7.** Polarized phosphorescence and excitation spectra of the pinacol dimer in ethanol glass at 77 K. The degree of polarization,  $(I_{\parallel} - I_{\perp}) / (I_{\parallel} + I_{\perp})$ , is negative with respect to the  $y$ -axis (the axis perpendicular to the  $C_2$  as well as the long in-plane axes of the naphthalene moieties) polarized  $^1B_2 \leftarrow ^1A_1$  absorption (ref 22) at about 325 nm and positive with respect to the  $z$  ( $C_2$ )-axis polarized  $^1A_1 \leftarrow ^1A_1$  band (ref 22) at about 280 nm. The results demonstrate that the phosphorescence is polarized along the  $Z$  ( $C_2$ ) axis of the dimer, consistent with the spin-orbit coupling scheme of Figure 6. The axes convention in Figures 6 and 7 differs from that used for the principal values of the ZFS tensor, Figure 4.

of the different emission characteristics (i.e., spectral position, vibronic structure, and lifetime; section IIIa) of the Agosta and pinacol dimers relative to those of the diketone and endoxy dimers. We may therefore conclude that the binding in the L-shaped  $T_1$  dimers comes from vdW energies as well as excitation exchange energies (Figure 5). Since both the vdW and excitation exchange interactions lower the energy of the  $T_1$  dimer relative to the  $T_1$  monomer, they will contribute to the red shift of the dimer phosphorescence (0.3–0.4 eV for the endoxy and diketone dimers and about 0.1 eV or less for the Agosta and pinacol dimers), along with the geometry change accompanying the excimer formation (vide infra).

Interestingly, the  $T_1$  tilt angles of the endoxy and diketone dimers, as determined from TREPR (Table 2), are substantially smaller than the tilt angle for the pinacol dimer. The tilt angles for the two dimers, exhibiting excimeric phosphorescence, are in fact about 10–20° smaller than the  $S_0$  tilt angles (110–120°) deduced from molecular modeling and quantum chemistry programs. The result implies that a major conformational change accompanying electronic excitation of the L-shaped dimers into  $T_1$  is the decrease in the tilt angle (i.e., increased puckering).

The strong red shift of the phosphorescence in going from more viscous to less viscous glasses, section IIIa, is consistent with this supposition. Such conformational change, leading to an increased intermolecular interaction, would be easier in the more flexible molecules than in the less flexible molecules. A recent quantum chemistry calculation on the Agosta dimer, using density functional (B3LYP) theory, also shows that the tilt angle is about 10° smaller in the optimized  $T_1$  geometry ( $\sim 110^\circ$ ) than in the optimized ground-state geometry ( $\sim 120^\circ$ ).<sup>22</sup>

As the vdW forces are not expected to be strongly affected by small changes in tilt angle, the greater red shift and shorter lifetime of phosphorescence for the diketone and endoxy dimers imply that the  $T_1(\pi\pi^*)-S_0$  as well as  $T_1(\pi\pi^*)-S_n$  ( $n > 1$ ) spin-orbit couplings are significantly greater for the L-shaped dimers with smaller tilt angle. The short  $T_1$  lifetime (assumed to be determined largely by  $T_1 \rightarrow S_0$  intersystem crossing<sup>17</sup>) is consistent with the  $^3B_2$  ( $T_1$ )– $^1A_1$  ( $S_0$ ) spin-orbit coupling in the  $C_{2v}$  dimers, see Figure 6, which is expected to be most efficient when the p orbitals on the two monomers are oriented perpendicular to each other (i.e., 90° tilt angle).<sup>27</sup> The  $T_1 \rightarrow S_0$  radiative decay rate would also be much greater in the L-shaped

dimers relative to the monomer, since the  $T_1 \rightarrow S_0$  radiative transition can gain considerable intensity from the spin-allowed  $S_2 (^1A_1) \rightarrow S_0 (^1A_1)$  transition via the  $T_1 (^3B_2) - S_2 (^1A_1)$  spin-orbit coupling, Figure 6. Consistent with such coupling scheme, the phosphorescence of the pinacol dimer is polarized parallel to the transition moment of the  $L_a (^1A_1 \leftarrow ^1A_1)$  band at about 280 nm, which lies along the  $C_2(z)$  axis of the  $C_{2v}$  dimer,<sup>17</sup> Figure 7. The greatly enhanced  $T_1 - S_0$  transition moment will lead to a large increase in the excitation resonance in  $T_1$  (which scales with the square of the  $T_1 - S_0$  transition moment) and contribute to the red shift of the phosphorescence spectrum of the L-shaped dimer relative to that of the monomer. The strong dependence of the excitation resonance on the tilt angle is indicated by the ZINDO calculation on the B3LYP geometry,<sup>22</sup> which shows that the exciton splitting in  $T_1$  increases by an order of magnitude when the tilt angle is decreased from 120° to 110°.

We conclude this section with a remark on the major difference between the phosphorescence of the L-shaped dimers and that of the face-to-face sandwich dimers of  $D_{2h}$  symmetry. As described in section IIIa, both the covalently linked and unlinked sandwich dimers of naphthalene exhibit phosphorescence that resembles the monomer emission, with respect to spectral position, vibronic structure, and lifetime. This observation suggests that the spin-orbit coupling, and hence the  $S_0 \rightarrow T_1$  transition moment, is substantially smaller in the face-to-face dimers as compared to the L-shaped dimers. This conclusion is consistent with the presence of a center of symmetry in the  $D_{2h}$  dimer which precludes spin-orbit coupling of  $T_1 (^3B_{3g})$  with the  $\pi\pi^*$  singlet state of ungerade (u) symmetry,<sup>22</sup> to which the electric dipole transitions from the ground ( $^1A_g$ ) state are allowed, Figure 6. The binding in the triplet excimer of sandwich conformation may therefore result almost entirely from the vdW forces (especially the attractive dispersion term). The similarity of the vibronic structure, polarization, and lifetime, of the phosphorescence between naphthalene and the sandwich dimers is in accord with the assumption that the spin-orbit coupling as well as the Franck-Condon factors for  $T_1 \rightarrow S_0$  radiative, and nonradiative, transitions are not significantly different for the  $D_{2h}$  dimers as compared to the monomer.

## V. Conclusion

There are several interesting conclusions that emerge from the studies of the L-shaped dimers of naphthalene described herein. First, the analyses of the TREPR data shows that the large decrease in the  $D$  values relative to the triplet monomer is consistent with the dimer geometries if it is assumed that the dominant source of this decrease is the excitation exchange interaction. The tilt angle between the planes of the two naphthalene systems appears to be about 10° smaller in the lowest triplet state relative to the ground state. Second, comparison of the tilt angles deduced from TREPR with the spectral position and lifetime of the phosphorescence, indicate that the excitation exchange interaction is large for dimers with smaller tilt angles, as compared to those with larger angles or with sandwich dimers. The proposal that the preferred conformation of the triplet excimer of naphthalene (and related compounds) is L-shaped, rather than sandwich, is supported by the measurements. Third, while the observation of strongly red shifted phosphorescence, with vibronic structure distinctly different from that of the monomer phosphorescence, is an indication of the intermolecular interaction (exciton resonance and

charge resonance) leading to triplet excimer formation, the observation of monomeric emission with small red shift is not a conclusive evidence for the absence of such interaction. This is illustrated by the observation that the sandwich dimers and the Agosta dimers, exhibiting monomeric phosphorescence at 77 K, display intermolecular CT absorption characteristic of triplet excimers.

**Acknowledgment.** Much of the work described in this paper were carried out about 10 years ago. We are grateful to Drs. Joseph Dresner and Steve Modiano for their experimental contributions and to Professors Noboru Hirota and Hans van Willigen for helpful discussions. This work was supported by the Office of Basic Energy Sciences of the U.S. Department of Energy.

## References and Notes

- (1) Hirayama, F. *J. Chem. Phys.* **1965**, *42*, 3163.
- (2) Chandross, E. A.; Dempster, C. J. *J. Am. Chem. Soc.* **1970**, *92*, 704.
- (3) Konijnenberg, E. Doctoral Thesis, Free University of Amsterdam, Holland, 1963.
- (4) Murrell, J. N.; Tanaka, J. *Mol. Phys.* **1964**, *45*, 363.
- (5) Azumi, T.; Armstrong, A. T.; McGlynn, S. P. *J. Chem. Phys.* **1964**, *41*, 3839.
- (6) Vala, M. T.; Hiller, I. H.; Rice, S. A.; Jortner, J. *J. Chem. Phys.* **1966**, *44*, 23.
- (7) (a) Chandra, A. K.; Lim, E. C. *J. Chem. Phys.* **1968**, *48*, 2589. (b) Chandra, A. K.; Lim, E. C. *J. Chem. Phys.* **1968**, *49*, 5066.
- (8) Lim, B. T.; Lim, E. C. *J. Chem. Phys.* **1983**, *78*, 5266.
- (9) Modiano, S. H.; Dresner, J.; Lim, E. C. *Chem. Phys. Lett.* **1992**, *189*, 144.
- (10) (a) Modiano, S. H.; Dresner, J.; Lim, E. C. *J. Phys. Chem.* **1991**, *95*, 9144 and earlier references therein. (b) Modiano, S. H.; Dresner, J.; Lim, E. C. *J. Phys. Chem.* **1993**, *97*, 3480.
- (11) Lim, E. C.; Locke, R. J.; Lim, B. T.; Fujioka, T.; Iwamura, H. *J. Phys. Chem.* **1987**, *91*, 1298.
- (12) (a) Dresner, J.; Modiano, S. H.; Lim, E. C. Unpublished results, 1989. (b) Cai, J.; Lim, E. C. Unpublished results, 1991.
- (13) Wang, X.; Kofron, W. G.; Kong, S.; Rajesh, C. S.; Modarelli, D. A.; Lim, E. C. *J. Phys. Chem.*, in press.
- (14) Agosta, W. C. *J. Am. Chem. Soc.* **1967**, *89*, 3505.
- (15) Cai, J.; Lim, E. C. *J. Phys. Chem.* **1990**, *94*, 8387.
- (16) Hirota, N.; Yamauchi, S.; Terazima, M. *Rev. Chem. Intermed.* **1987**, *8*, 189.
- (17) Cai, J.; Lim, E. C. Unpublished results, 1990.
- (18) Tero-Kubota, S.; Miyamoto, T.; Akiyama, K.; Ikegami, Y.; Mataka, S.; Tashiro, M. *Chem. Phys. Lett.* **1996**, *249*, 314.
- (19) Yanagidate, M.; Takayama, K.; Takeuchi, M.; Nishimura, J.; Shizuka, H. *J. Phys. Chem.* **1993**, *97*, 8881.
- (20) Ishikama, S.-I.; Nakamura, J.; Iwata, S.; Sumitani, M.; Nagakura, S.; Sakata, J.; Misumi, S. *Bull. Chem. Soc. Jpn.* **1979**, *52*, 1346.
- (21) Murov, S. L.; Carmichael, I.; Hug, G. L. *Handbook of Photochemistry*, 2nd ed.; Marcel Dekker: New York, 1993 and references therein.
- (22) East, A.; Lim, E. C. To be published.
- (23) Dresner, J.; Modiano, S.; Cai, J.; Lim, E. C. Unpublished result, 1989.
- (24) Yamaji, M.; Shima, K.; Nishimura, J.; Shizuka, H. *J. Chem. Soc., Faraday Trans.* **1997**, *93* (6), 1065.
- (25) See, for example: Scholes, G. D.; Ghiggino, K. P. *J. Phys. Chem.* **1994**, *98*, 4580.
- (26) A rough estimate of the energy gap can be made as follows. The energy of the CT state can be deduced from  $E(D^+A^-) = E_{ox}(D/D^+) - E_{red}(A^-/A) + 0.15$  eV, which is valid for *n*-hexane (Weller, A. In *The Exciplex*; Gordon, M.; Ware, W. R., Eds.; Academic Press: New York, 1975; p 113). Using  $E(D/D^+) = 1.67$  eV (vs SCE) and  $E(A^-/A) = -2.54$  eV, we obtain 4.36 eV for the energy of the CT state. The energy gap between the CT state and the lowest triplet state ( $E = 2.64$  eV) is therefore about 1.72 eV for naphthalene in *n*-hexane.
- (27) The spin-orbit coupling between the  $^3B_2$  and  $^1A_1$  states occurs through the  $R_x(b_2)$  component of the orbital angular momentum operator, where  $x$  axis lies parallel to the in-plane long axes of the monomers and  $z$  is the  $C_2$  axis of the  $C_{2v}$  dimer (Note that this axes convention differs from that used for the principal values of the ZFS tensor, Figure 4).